


## Article

# Partitioning of Dissolved Organic Carbon, Major Elements, and Trace Metals during Laboratory Freezing of Organic Leachates from Permafrost Peatlands

Irina S. Ivanova<sup>1</sup>, Liudmila S. Shirokova<sup>1,2</sup>, Jean-Luc Rols<sup>3</sup> and Oleg S. Pokrovsky<sup>4,5,\*</sup> 

- <sup>1</sup> Tomsk Branch of the Trofimuk Institute of Petroleum Geology, Geophysics of Siberian Branch, Russian Academy of Sciences, 4 Akademicheskoy Pr., 634021 Tomsk, Russia; ivanovais\_1986@mail.ru (I.S.I.); lshirokova@yandex.ru (L.S.S.)
- <sup>2</sup> N. Laverov Federal Center for Integrated Arctic Research, Ural Branch of the Russian Academy of Sciences, 23 Nab Severnoi Dviny, 163000 Arkhangelsk, Russia
- <sup>3</sup> Laboratoire Ecologie Fonctionnelle et Environnement, CNRS, Toulouse INP, Université Toulouse 3—Paul Sabatier (UPS), 31062 Toulouse, France; jean-luc.rols@univ-tlse3.fr
- <sup>4</sup> BIO-GEO-CLIM Laboratory, Tomsk State University, 35 Lenina Pr., 634510 Tomsk, Russia
- <sup>5</sup> Geosciences and Environment Toulouse, UMR 5563 CNRS, University of Toulouse, 14 Avenue Edouard Belin, 31400 Toulouse, France
- \* Correspondence: oleg.pokrovsky@get.omp.eu; Tel.: +33-561-332-625

**Featured Application:** Elaboration of unified experimental protocol for studying freezing and thawing of organic-rich (humic) natural waters under laboratory conditions.

**Abstract:** Climate change is likely to modify the freezing–thawing cycles in soils and surface waters of permafrost-affected and subarctic regions. However, the change of solution chemical composition during ice formation and the evolution of the remaining fluids remain very poorly known. Towards a better understanding of dissolved (<0.45 µm) organic carbon, as well as major and trace element behavior in permafrost peatland environments, here we performed laboratory freezing of peat leachates, from complete freezing to complete thawing, in order to quantify the partitioning of solutes between the aqueous solution and the remaining ice. Freezing experiments were conducted, with and without polyurethane insulation. Two main types of experiments involved (i) progressive freezing, when we started from liquid leachates (filtered <0.45 µm) and allowed them to freeze at −18 °C, and (ii) progressive thawing, where first, we froze solid a series of <0.45 µm filtered leachates and then monitored their thawing at room temperature, 20 °C. We hypothesized the existence of two main groups of solutes, behaving conservatively or non-conservatively during freezing, depending on their incorporation into the ice or their ability to coagulate in the form of insoluble minerals or amorphous materials in the fluid phase. An unexpected result of this work was that, despite a sizable degree of element concentration in the remaining fluid and possible coagulation of organic, organo-mineral, and inorganic compounds, the freezing and subsequent thawing produced final concentrations of most solutes which were not drastically different from the initial concentrations in the original leachates prior to freezing. This demonstrates the high stability of dissolved (<0.45 µm) organic carbon, iron, aluminum, and some trace metals to the repetitive freezing and thawing of surface waters in permafrost peatlands.

**Keywords:** peat; freezing; thawing; major; trace elements; organic carbon; experiments



**Citation:** Ivanova, I.S.; Shirokova, L.S.; Rols, J.-L.; Pokrovsky, O.S. Partitioning of Dissolved Organic Carbon, Major Elements, and Trace Metals during Laboratory Freezing of Organic Leachates from Permafrost Peatlands. *Appl. Sci.* **2023**, *13*, 4856. <https://doi.org/10.3390/app13084856>

Academic Editors: Kai-Qi Li, Jun Hu and Jie Zhou

Received: 10 March 2023

Revised: 11 April 2023

Accepted: 11 April 2023

Published: 12 April 2023



**Copyright:** © 2023 by the authors. Licensee MDPI, Basel, Switzerland. This article is an open access article distributed under the terms and conditions of the Creative Commons Attribution (CC BY) license (<https://creativecommons.org/licenses/by/4.0/>).

## 1. Introduction

The climate warming in high latitudes leads to the change in frequency of the seasonal thawing-freezing regime [1,2] which will be mostly pronounced during autumn and spring, i.e., the so called “shoulder” seasons or transition periods [3]. It is known that spring and autumn are extremely important for the export of dissolved and particulate load by

rivers and element cycling in the lakes of Arctic wetlands [4–6]. During these transition periods, the majority of organic carbon and inorganic solutes originate from leaching of supra-permafrost soil and vegetation [7,8]. In addition to the effect on the carbon and major elements cycling, these processes largely control the release of many trace elements from soils to the aquatic systems [5,9,10]. However, in contrast to relatively good empirical and modeling understanding of the physical aspects of soil freeze/thaw processes [1,11], the behavior of aqueous solutes (<0.45  $\mu\text{m}$ ) upon freezing and thawing of organic matter-rich surface and soil waters of permafrost peatlands remains poorly understood. It is known that both the peat porewaters [12,13] and surface waters [5,7] of these regions are strongly enriched in dissolved organic carbon (DOC) and some trace metals. These solutes are often present in the form of organic and organo-mineral colloids [10,14,15], which are likely to coagulate upon ice formation, for example, during the full freezing of surface depressions and shallow thermokarst lakes and ponds [4]. In contrast to the sizable number of works devoted to characterizing the impact of freezing and thawing on mineral soil properties [16–34], the freezing/thawing impact on the chemical composition of porewater and ice has not been well described, and most often, the researchers have to rely on modeling predictions [35].

Although laboratory experiments allow for the identification of governing factors during freezing/thawing effects [36–43], their applications to naturally relevant aquatic settings of high latitude permafrost peatlands remain very restricted. Previous works in permafrost peatlands reported translocation of microorganisms and changes in porewater chemistry (pH, UV absorbance, DOC, major and trace element concentrations) after the thawing and bidirectional freezing of peat cores [44,45]. Another recent study examined the impact of freezing/thawing cycles (FTC) on the surface waters from Northeast European permafrost peatland [46]. The latter authors reported only minor (<5–15%) changes of DOC and labile ion concentrations, whereas several trace elements (Fe, Al, P, Mn, As, and REE) exhibited a sizable decrease in their concentrations after FTC. These authors concluded an overwhelming impact of colloidal status of DOC and trace metal on this coagulation/dissolution processes during freezing and thawing. However, the quantitative assessments of these effects are still missing. In the present study, we aimed at (1) elaborating an optimal experimental procedure allowing for a discrete sampling of fluid during complete freezing progress; (2) quantifying the partitioning coefficients of elements between water and ice, and (3) testing the relationship between different elements, depending on their speciation and affinity to dissolved organic matter.

We hypothesize the existence of several group of contrasting solutes—(1) those incorporating into forming ice; (2) those remaining in the fluid phase via concentrating due to freezing front migration but not subjected to coagulation, and (3) less soluble complex organo-mineral amorphous compounds or certain minerals, subjected to reversible or irreversible coagulation. Testing these mechanistic hypotheses constituted the first objective of this study. The second objective was to use laboratory leachates of natural substrates (peat) as surrogates for the direct experimental modeling of chemical and physical processes occurring in shallow surface waters and topsoil horizons during the autumn—spring period. We anticipate that achieving these objectives should allow a uniform approach for the laboratory modeling of natural aquatic processes in permafrost peatlands and provide useful background for assessing the impact of climate change on chemical composition of surface waters in these environmentally-important regions.

## 2. Materials and Methods

### 2.1. Organic Substrates from Permafrost Peatlands Used for Aqueous Leachate Preparation

Peat core samples were collected at the end of the summer in the two largest permafrost peatlands of Northern Eurasia—the Bolshezemelskaya Tundra (NE Europe) and the Western Siberia Lowland (Figure 1). Two peat horizons, thawed (surface, 0 to 10 cm) and deep (frozen, between 40 and 50 cm) were collected from at the sampling sites is between 30 and 40 cm, and the permafrost is discontinuous. The dominant vegetation on

the mound is mosses and lichens, with some dwarf shrubs. The detailed description of the environmental context of the sampling sites is provided elsewhere (for Bolshezemelskaya Tundra [47,48] and for Western Siberia [49,50]).

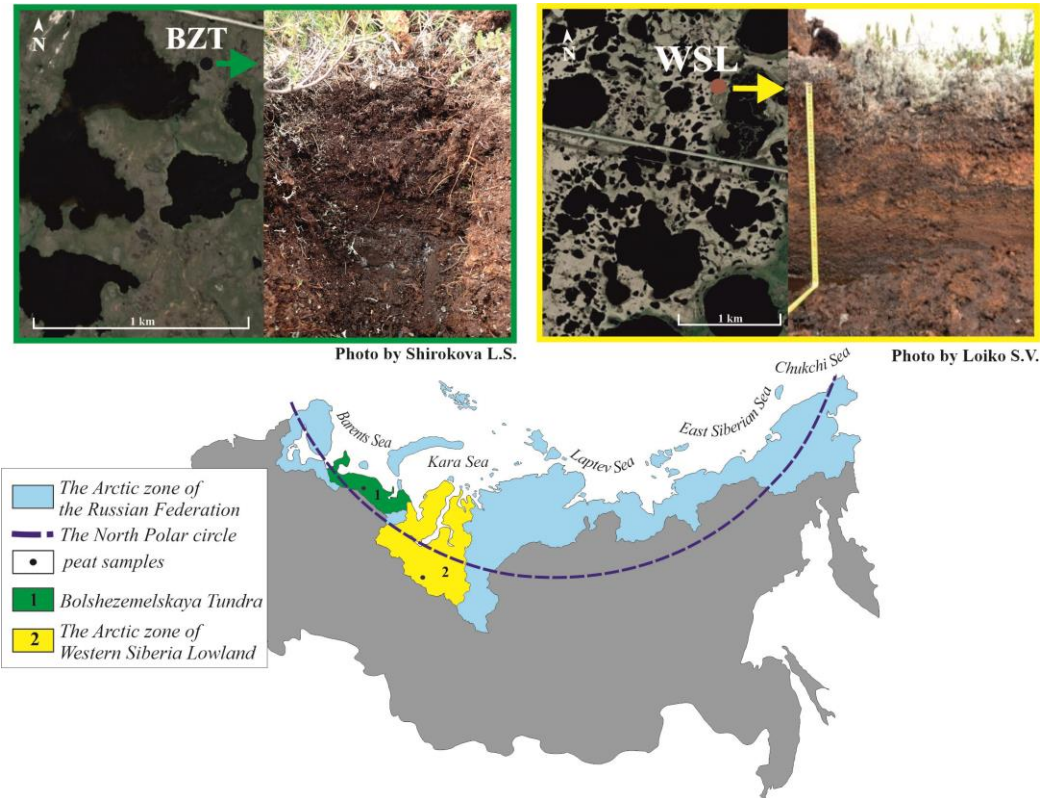


**Figure 1.** Location map of study area in the Bolshezemelskaya Tundra (1, BZT) and the Western Siberia Lowland (2, WSL), along with photos of sampled peat cores and their environmental context (flat-mound bogs with thermokarst lakes).

To prepare aqueous leachates, 10 g of dry sample (thawed and frozen peat) was reacted in a shaker at 25 °C with 1 L of Milli-Q water for 24 h under aerobic conditions, with periodic aeration. The resulting suspension was filtered through a sterile single-use Millipore filter unit and placed in broad mouth, PES jars of 150 mL volume.

## 2.2. Freezing Experiments of Aqueous Leachates

Freezing experiments were conducted in two main setups: with polyurethane insulation (approximately 10 cm around the jars and the bottom), and without insulation, as illustrated in Figure 2. Inside the plastic jar, we placed a flexible tube which was connected to a syringe and which allowed for the sampling of fluid in the course of the experiment. The freezing occurred from the borders to the center of the jar, in the case of no insulated reactors, and from the surface to the bottom, in the case of insulated reactors (Figure 2). As such, the sampling tube was located at the center of the jar, for the non-insulated reactors, and at the bottom of the jar, in case of the insulated reactors.

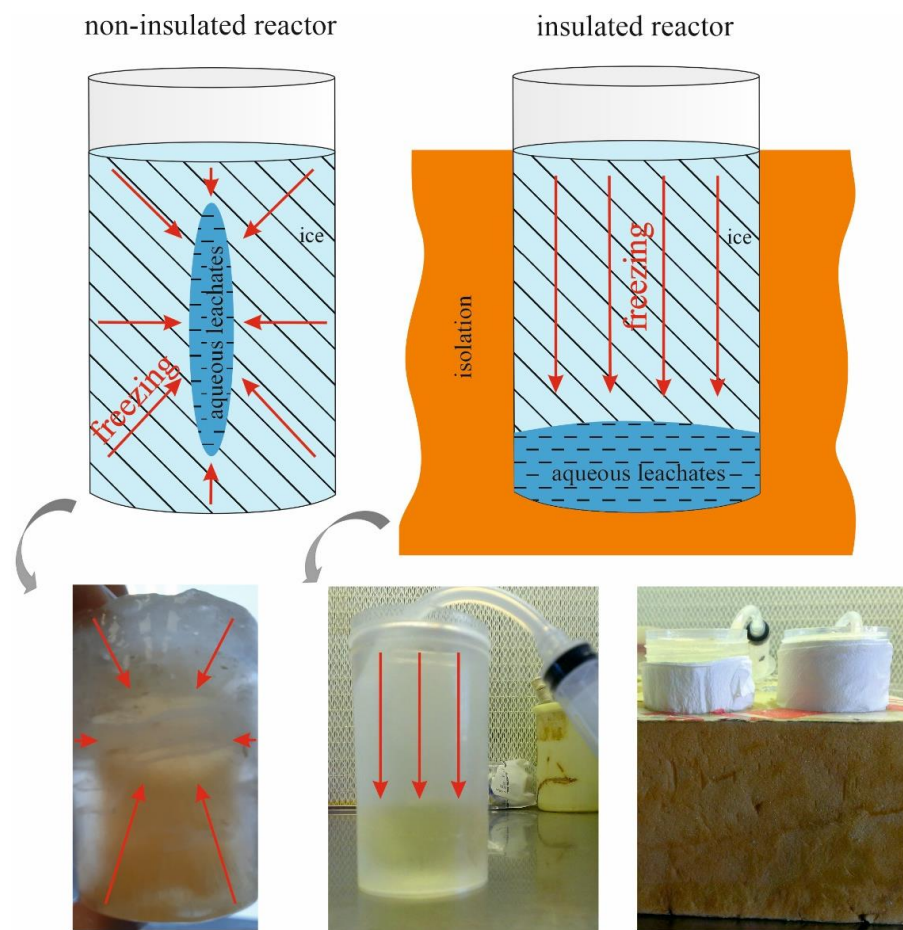


**Figure 2.** A scheme of experiments and photos of experimental reactors.

The two main type of experiments involved (i) progressive freezing, in which we started from liquid leachates (filtered  $<0.45\ \mu\text{m}$ ) and allowed them to freeze at  $-18\ ^\circ\text{C}$ , and (ii) progressive thawing, in which we first froze solid a series of  $<0.45\ \mu\text{m}$  filtered leachates, and then monitored their thawing at room temperature,  $20\ ^\circ\text{C}$ . In order to avoid the change in the fluid: ice ratio during sampling, we used a single-reactor sacrificial sampling technique. For this, instead of consecutive sampling from the same reactor, 10 identical reactors with filtered leachates were prepared simultaneously and placed in the freezer. Each sampling used the entire reactor, which was then removed from the freezer and discarded.

The sampling was performed regularly as follows. Samples of the aqueous leachate of peats with an insulant were taken after 6, 8, 11, and 15 h, whereas samples of the aqueous leachate of peat BZT were taken after 6, 11, 29, and 31 h. Samples of the aqueous leachate of peats without insulant were taken after 4, 5, and 6 h, and samples of aqueous leachate of peat BZT were taken after 4 and 5 h. During the thawing of the aqueous leachate of WSL peat, samples were collected after 2, 3, and 6 h, and samples of the aqueous leachate of peat BZT were collected after 1, 2, 3, 5, and 7 h. Typically, between 30 and 50% of the remaining or formed fluid was collected; the volume of sampled fluid did not exceed 15% of the initial volume. Immediately before sampling, the reactors were vigorously shaken to homogenize the precipitate that could have been formed in the remaining fluid. This guaranteed the avoidance of the dilution or concentration of solutes relative to precipitates formed during the freezing of peat leachates.

### 2.3. Chemical Analyses

A non-filtered subsample of the fluid which was extracted from freezing reactor was used to measure pH (uncertainty of  $\pm 0.01$  pH units, WTW inoLab-pH7110) and specific conductivity ( $\pm 0.1 \mu\text{S cm}^{-1}$ , Consort C830). The rest of the 15 mL was filtered through a  $0.45 \mu\text{m}$  Minisart<sup>®</sup> (Fisher Scientific, Illkirch-Graffenstaden, France) syringe filter. In the  $<0.45 \mu\text{m}$  filtrates, the DOC and DIC were analyzed by high-temperature catalytic oxidation using TOC-VCSN, Shimadzu<sup>®</sup> (Genzo Shimadzu Sr., Kyoto, Japan), with an uncertainty of  $\pm 2\%$  and a detection limit of  $0.1 \text{ mg L}^{-1}$ . The DIC was measured after sample acidification with HCl, and the DOC was analyzed in the acidified samples after sparging with C-free air for 3 min at  $100 \text{ mL min}^{-1}$  as non-purgeable organic carbon (NPOC). The internationally certified water samples (MISSISSIPPI-03) were used to check the validity and reproducibility of the analysis. The UV-absorbance of the water samples was measured using a 10 mm quartz cuvette on a CARY-50 UV-Vis spectrophotometer (Varian, Belrose, Australia) to assess the aromaticity of pore fluids via specific UV absorbance ( $\text{SUVA}_{254}$ ). Major cations, Si, P, and ~40 trace elements (TE) were measured in He and Ar operating modes, with a quadrupole ICP-MS Agilent 7500 ce (Agilent Technologies, Santa Clara, CA, USA). Indium and rhenium (approximately  $3 \mu\text{g L}^{-1}$ ) were used as internal standards to correct for instrumental drift and eventual matrix effects. The appropriate corrections for oxide and hydroxide isobaric interferences were applied for the Rare Earth Elements (REE). Three in-house standard solutions (1, 10, and  $100 \mu\text{g L}^{-1}$  of each element in 2%  $\text{HNO}_3$ ) were measured every 10 samples. The data tables present the results for the elements, exhibiting a good agreement ( $\pm 10\%$ ) between the certified or recommended values and our measurements, or for cases in which we obtain a good reproducibility (the relative standard deviation of our various measurements of standards lower than 10%), even if no certified or recommended data are available. During ICP MS analysis, the SLRS-5 international standard [51,52] was measured at the beginning of the analytical session and after each 20 samples to assess the external accuracy and sensitivity of the instrument. All certified major (Ca, Mg, K, Na, Si) and trace elements (Al, As, B, Ba, Co, Cr, Cu, Fe, Ga, Li, Mn, Mo, Ni, Pb) and all naturally-occurring REEs (La, Ce, Pr, Nd, Sm, Eu, Gd, Dy, Ho, Er, Tm, Yb, Lu, Sb, Sr, Th, Ti, U, V, Zn) concentrations of the SLRS-5 standard and the measured concentrations agreed, with an uncertainty of 10–20%. The agreement for Cd, Cs, and Hf was between 30 and 50%. For all major and most trace elements, the concentrations in the blanks were below analytical detection limits ( $\leq 0.1\text{--}1 \text{ ng L}^{-1}$  for Cd, Ba, Y, Zr, Nb, REE, Hf, Pb, Th, U;  $1 \text{ ng L}^{-1}$  for Ga, Ge, Rb, Sr, Sb;  $\leq 10 \text{ ng L}^{-1}$  for Ti, V, Cr, Mn, Fe, Co, Ni, Cu, Zn, As). Some rare elements, such as Sn, Nb, W, Tl, Ta, and Bi, which were not certified in the reference materials, were also measured, but their concentrations were presented only in the case when three independent subsamples provided a  $<20\%$  agreement.

### 2.4. Data Interpretation

In order to identify the group of solutes depending on their partitioning between the forming ice and the remaining solution, we normalized the concentration of main non-conservative solutes (DOC, Fe, Al, P, Mn, Sr, trivalent and tetravalent hydrolysates) to that of major and inert components which were not subjected to coagulation/mineral precipitation, such as K, Na, or Cl. Note that we could not use Mg, Ca, Si, and sulfate for such a normalization because these ions can form sparingly soluble salts (Mg, Ca carbonates, Ca sulfate, Mg hydrous silicate) upon progressive concentration of the remaining fluid during freezing. Assuming that there is no (or very little) incorporation of soluble labile ions into the ice structure, we calculated the degree of element accumulation in the remaining fluid at each time ( $C_t$ ) relative to the initial concentration ( $C_0$ ), i.e., the element concentration factor ( $F_{\text{conc}}$ ), as follows:

$$F_{\text{conc}} = C_t/C_0. \quad (1)$$

To differentiate between conservative and non-conservative elements, the  $F_{\text{conc}}$  value of each element at each time  $t$  of sampling was normalized to that of Na and traced as a function of time for each consecutive sampling.

### 2.5. Statistical Analysis

The data were processed by means of mathematical statistics using the MS Excel and Statistica software (version 13.2, Microsoft) at a significance level value of 5%. Additionally, in order to better differentiate between groups of elements, we performed pairwise (Pearson) correlations between elements in the fluid phase, considering all substrates and all types of treatments together. Significance criterion was set at  $p < 0.05$ . Significance of the difference in element concentration between different experimental treatments (freezing and thawing; with and without isolation; surface and deep peat horizon; peat from NE European tundra and Western Siberia) was examined by a pairwise Mann–Whitney test at  $p < 0.05$ .

## 3. Results

### 3.1. Initial Leachate Composition and the Impact of Reactor Design and Freezing Mode on Element Concentration in the Remaining Fluid

There were significant differences in element concentrations in the initial leachate of frozen and thawed peat horizons, as well as between the peat of NE European tundra (BZT) and Western Siberia (WSL). Thus, the leachates of peat from the NE European Tundra demonstrated sizably lower pH than those of the WSL (4.74 and 5.8–6.2, respectively), with a 2.5 times higher DOC concentration (Table 1).

**Table 1.** Element concentrations in the initial leachates (<0.45  $\mu\text{m}$ ) of frozen peat from NE European tundra (BZT) and frozen and thawed peat horizons of Western Siberia (F WSL and WSL, respectively).

Element	Western Siberian Lowland		European Tundra	Element	Western Siberian Lowland		European Tundra
	WSL	F WSL	BZT		WSL	F WSL	BZT
S.C., $\mu\text{S cm}^{-1}$	10	20	15.5	Zr, $\mu\text{g/L}$	0.0192	0.0878	0.4806
UV <sub>245</sub> , nm	0.386	0.167	1.037	Nb, $\mu\text{g/L}$	0.0015	0.0007	0.0095
pH	5.78	6.2	4.74	Mo, $\mu\text{g/L}$	0.1083	0.9193	0.034
DOC, mg/L	9.1	8.0	27.4	Cd, $\mu\text{g/L}$	0.0607	0.0579	0.0045
Li, $\mu\text{g/L}$	0.01	0.01	NA	Sb, $\mu\text{g/L}$	0.0144	0.0566	0.007
B, $\mu\text{g/L}$	59.2	54.8	72.3	Cs, $\mu\text{g/L}$	0.0004	0.0004	0.0015
Na, $\mu\text{g/L}$	915	686	1472	Ba, $\mu\text{g/L}$	163.8	10.56	245
Mg, $\mu\text{g/L}$	73	8	150.3	La, $\mu\text{g/L}$	0.0214	0.0137	0.0375
Al, $\mu\text{g/L}$	15.6	9.8	78.1	Ce, $\mu\text{g/L}$	0.032	0.0277	0.069
Si, $\mu\text{g/L}$	32	19	388	Pr, $\mu\text{g/L}$	0.0031	0.0024	0.0084
P, $\mu\text{g/L}$	9.2	15.0	68.3	Nd, $\mu\text{g/L}$	0.0141	0.0096	0.0362
K, $\mu\text{g/L}$	215	113.3	732.5	Sm, $\mu\text{g/L}$	0.0049	0.0017	0.0101
Ca, $\mu\text{g/L}$	289	257.3	571.7	Eu, $\mu\text{g/L}$	0.0119	0.0011	0.0192
Ti, $\mu\text{g/L}$	0.106	0.1155	0.439	Gd, $\mu\text{g/L}$	0.0054	0.0031	0.0147
V, $\mu\text{g/L}$	0.360	0.2248	0.176	Tb, $\mu\text{g/L}$	0.0005	0.0003	0.0017
Cr, $\mu\text{g/L}$	0.040	0.06	0.460	Dy, $\mu\text{g/L}$	0.004	0.0023	0.0095
Mn, $\mu\text{g/L}$	1.26	0.1153	0.0323	Ho, $\mu\text{g/L}$	0.0007	0.0003	0.0017
Fe, $\mu\text{g/L}$	22.9	12.3	56.0	Er, $\mu\text{g/L}$	0.0068	0.0047	0.0058
Co, $\mu\text{g/L}$	0.015	0.0104	0.0373	Tm, $\mu\text{g/L}$	0.0005	0.0001	0.0009
Ni, $\mu\text{g/L}$	0.17	0.18	0.26	Yb, $\mu\text{g/L}$	0.0024	0.0009	0.0059
Cu, $\mu\text{g/L}$	0.674	0.7167	25.4	Lu, $\mu\text{g/L}$	0.0003	0.0002	0.0008
Zn, $\mu\text{g/L}$	212	8.62	420	Hf, $\mu\text{g/L}$	0.0019	0.0089	0.0343
Ga, $\mu\text{g/L}$	0.0002	0.0006	0.0181	W, $\mu\text{g/L}$	0.0069	0.0558	0.005
As, $\mu\text{g/L}$	0.1754	0.1352	0.2781	Pb, $\mu\text{g/L}$	0.044	0.025	1.406
Rb, $\mu\text{g/L}$	0.08	0.05	0.26	Th, $\mu\text{g/L}$	0.0019	0.0017	0.0204
Sr, $\mu\text{g/L}$	4.96	2.417	5.048	U, $\mu\text{g/L}$	0.0013	0.003	0.0074
Y, $\mu\text{g/L}$	0.0248	0.0114	0.0514				

Note: S.C.—specific conductivity.

As a result of such high acidity of organic-rich waters, the leachates of BZT peat were sizably, by a factor of 2 to 3, richer in Fe, Al, and other trace metals compared to those

from the WSL peat. The leachates from the active horizon of the WSL peat layer exhibited 0.4 unit lower pH values, 1.5 to 2.0 times higher concentrations of Si, K, Fe, Al, Sr, and 10–20 times higher Mn, Zn, and Ba levels than the leachates from the frozen peat horizons.

3.2. Evolution of pH, DOC, and Metal Concentration in the Fluid Phase during the Freezing and Thawing of Peat Leachates

Preliminary examination of the concentration evolution in the course of freezing and thawing (in both directions) demonstrated that there was no significant (at  $p < 0.05$ ) difference between the two treatments in terms of pH, DOC, major, and trace element concentration evolution. Progressive freezing of the aqueous peat leachates led to a decrease in pH relative to the initial solutions (Figure 3), as well as a general increase in DOC and element concentrations, but this increase was different among peat samples. Thus, a sizable—a factor of 2 to 3—increase in the concentration of most elements in the remaining fluid occurred during the freezing of leachates from the active (upper) layer peat of both Western Siberian (WSL) and NE European Tundra (BZT), shown as brown and black symbols, respectively, in Figure 3.

This was not the case for the leachates of frozen Siberian peat: this sample did not exhibit any systematic change in the concentration of solutes during progressive freezing and thawing (shown by blue symbols in Figure 3). Such a drastic difference in the behavior of the leachates from frozen and thawed peat horizons is not linked to pH or DOC behavior, but is likely due to the intrinsic properties of leachates, which depended on the position of the peat sample at the core, with respect to active layer depth.

Progressive thawing of completely frozen leachates produced a decrease in concentration after each subsequent sampling (shown as crosses in Figure 3); the curve approximating the element concentration versus time followed approximately that of progressive freezing. This was observed for most analyzed elements, including DOC, Fe, Al, P, some divalent trace metals, and trivalent and tetravalent hydrolysates.

We found that the initial concentration of some elements in leachates, prior to freezing, were not always recovered after full freezing and thawing of the reactors (Figure 4). This result is consistent with previous works on the freezing/thawing cycles of filtrates from northern peatlands that demonstrated a sizable coagulation and the removal of low-soluble elements bound to organic colloids [46,53].

Considering the element recovery from entire freezing/thawing cycle, three groups of elements could be distinguished separately for each substrate (Table 2).

**Table 2.** The degree of element recovery during the entire reversible freezing and thawing cycle, separately for <0.45 μm of leachates of peat from BZT, and from frozen (F WSL) and thawed (WSL). The significance of group distinction is at  $p < 0.05$  (Mann–Whitney test).

WSL	F WSL	BZT
	$C_0/C_{final} < 0.5$	
Li, Cu, Pb, Th, U	Mg, Mn, Zn, Cd, Ba	Mg, Al, Si, V, Mn, Fe, Co, Ni, Ga, Rb, Zr, Cd, Sb, Cs, Ce, Pb, Th
	$C_0/C_{final} 0.5-1.5$	
DOC, B, Na, Mg, Al, P, K, Ca, Ti, V, Cr, Mn, Fe, Co, Zn, Ga, As, Rb, Sr, Zr, Mo, Cd, Sb, Cs, Ba, REEs, Hf	Li, B, Na, Al, Ti, V, Fe, Co, Ni, Cu, Ga, Zr, Mo, Sb, Cs, Ba, REEs, Hf, Pb, U	DOC, B, Na, P, K, Ca, Ti, Cr, Cu, As, Sr, Mo, Ba, REEs, Hf, W
	$C_0/C_{final} 1.5-3$	
Si, Ni, Yb	DOC, K, Ca, As, Sr	U
	$C_0/C_{final} > 3$	
	P, Rb, Th	Zn

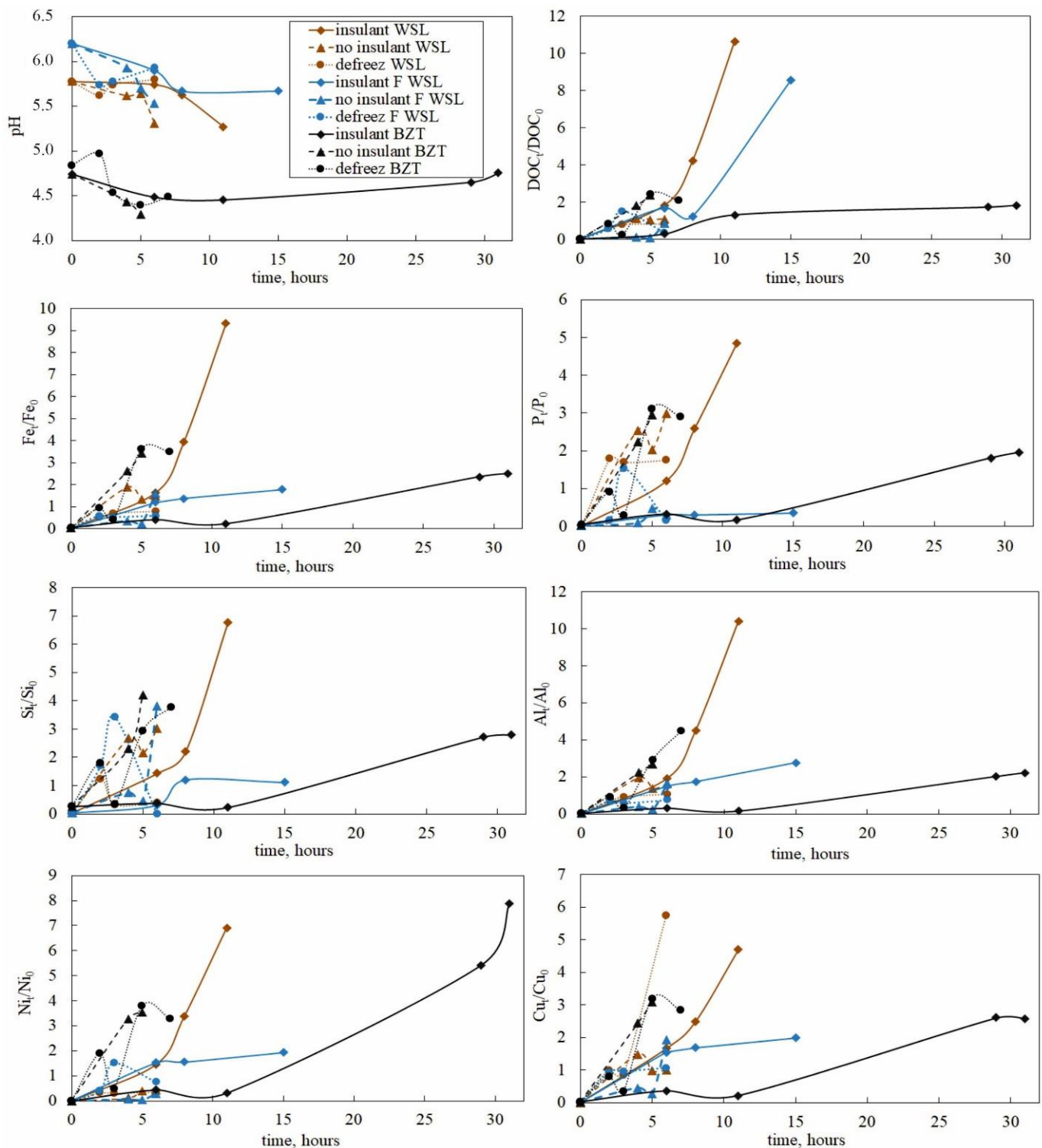


**Figure 3.** Temporal evolution of pH and solute (DOC, Fe, P, Si, Al, Ni, and Cu) concentrations in the remaining and forming fluid during progressive freezing and thawing, respectively, of peat leachates obtained from active (thawed) and permanently frozen (below active layer depth) peat horizons of permafrost peatlands in Northern Eurasia ( $p < 0.05$ ). Freezing is shown by diamonds and triangles, whereas thawing is shown by circles. The concentration of element at time  $t$  and initial (0) were normalized to that of sodium. Connecting lines are for guiding purposes. Analytical error bars are within the symbol size.



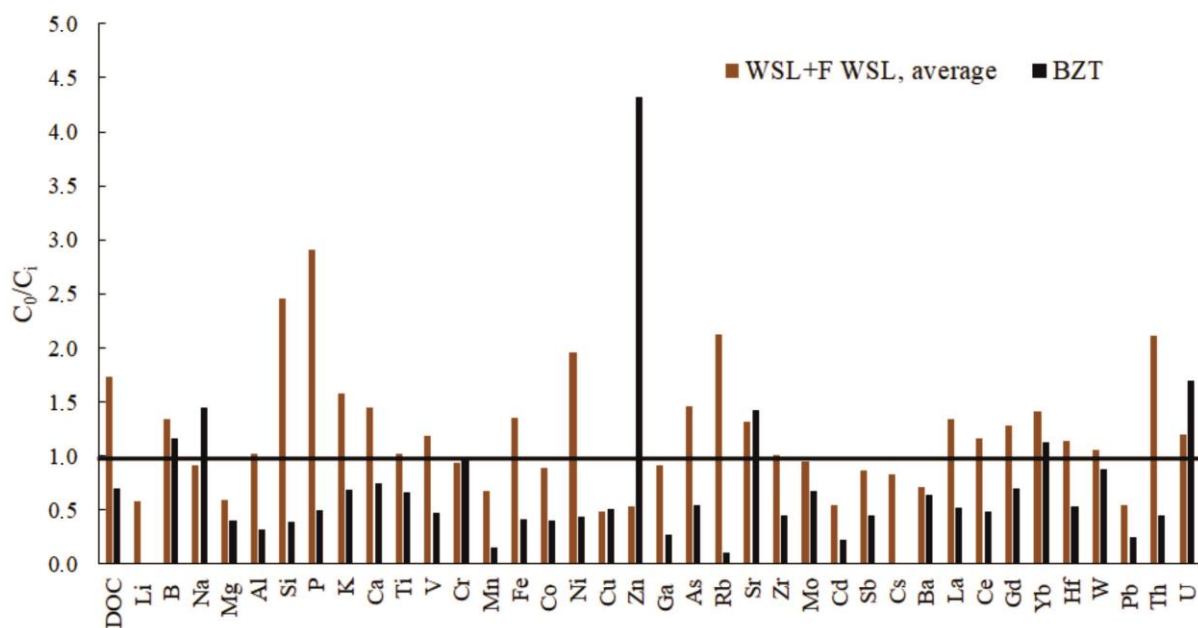


**Figure 4.** A histogram of ratios of the element concentration in the leachate prior to freezing ( $C_0$ ) to the final concentration after the entire freezing/thawing cycle. The values above 1 indicate some removal of an element in the form of coagulates. The values below 1 likely represent experimental/analytical artifacts. A significant (at  $p < 0.05$ ) difference from 1.0 is considered as a 30% deviation.

We discovered that the leachates from the frozen peat horizons (WSL) behaved differently from the leachates of the thawed horizons; namely, in the case of the leachate from frozen peat, the element concentration in the remaining fluid during progressive freezing did not increase significantly and remained rather constant over time. This contrasted with the temporal pattern of thawed peat leachates: the concentration of elements in the remaining fluid strongly increased upon freezing (Figure 3). This result could signify the efficient incorporation of solutes from frozen peat leachate into the forming ice, as reflected by the quite low partitioning coefficients of elements between the forming ice and the remaining fluid for this type of substrate. We have no explanation for the potential mechanism of the rather unexpected behavior of this particular leachate, but we can hypothesize that some volumes of the fluid, formed from the frozen leachate, partially preserved the peat dispersed ice structure and chemical composition (i.e., [9,10]) and could be directly incorporated into the forming ice, with a partitioning coefficient close to 1. Clearly, further freezing/thawing experiments, including the assessment of colloidal forms of aquatic leachates obtained from permanently frozen peat horizons (sampled below the active layer boundary) are needed to verify and develop this hypothesis.

### 3.3. Group of Elements Depending on Their Conservative and Non-Conservative Behavior during Freezing Revealed via Correlation Relationships

The correlations between element concentrations during freezing and thawing at different modes (with and without insulant, Figure 5 and Table 3) allowed for the distinguishing of two main groups of solutes: DOC, Fe, and Al as potential carriers of Si, P, K, Cr, Co, Ni, Cu, As, Pb, Nb, and trivalent and tetravalent hydrolysates, as well as Ca, Na, and K as major indicators of conservative solutes that did not exhibit any significant correlations with other solutes. It was found that while Fe, Al, and other trace metals, notably  $TE^{3+}$ , and  $TE^{4+}$ , exhibited strong correlations during freezing and thawing, the labile Na or Ca (as a major cation) did not correlate with Fe, Al, and DOC in any of the substrates. Note that the maximal number of elements correlated with three major components of the organo-mineral colloids (DOC, Fe, and Al) was observed in thawing rather than freezing experiments.

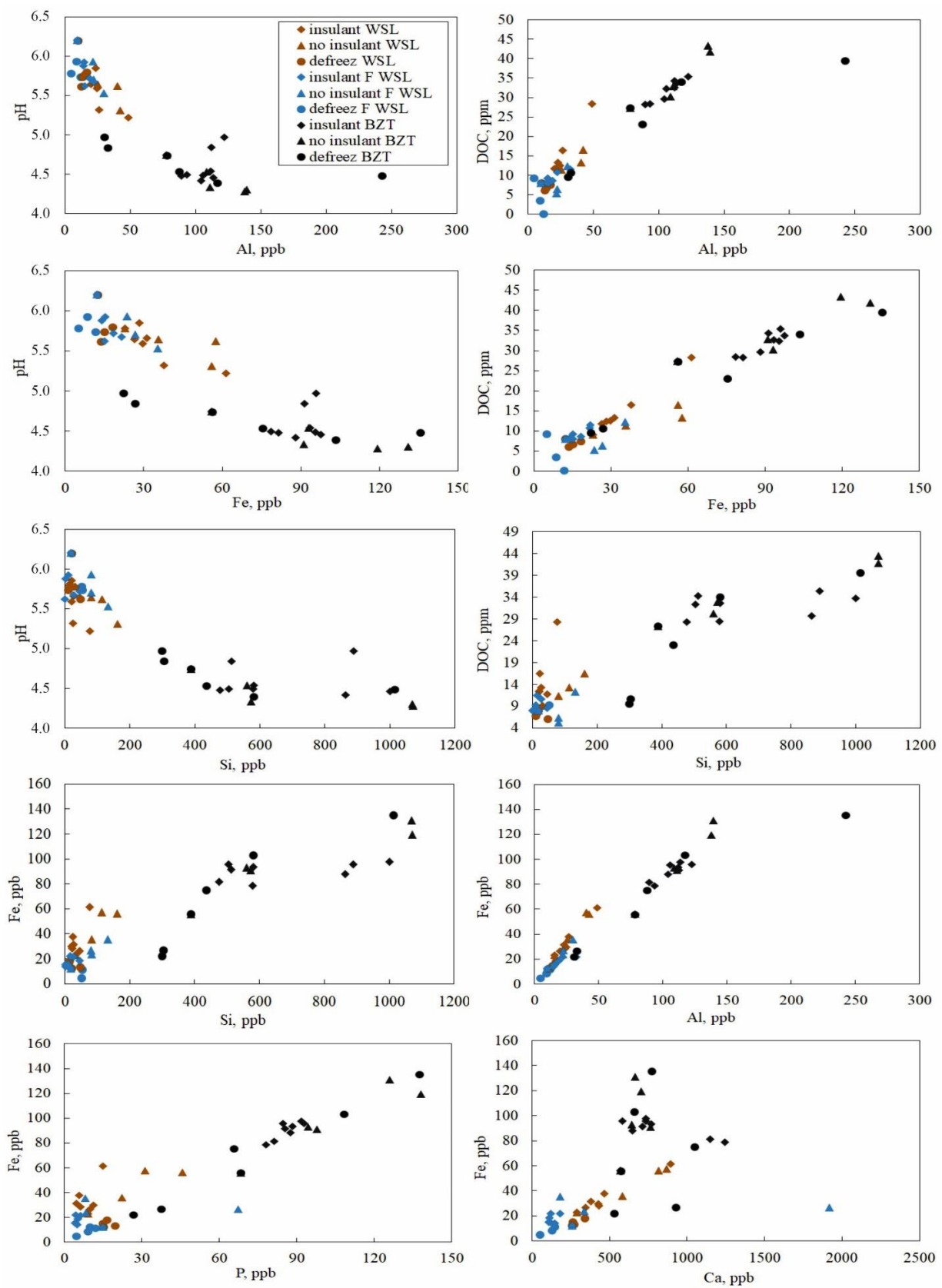


**Figure 5.** Examples of correlations between solute concentrations for all conducted experiments ( $p < 0.05$ ). Analytical error bars are within the symbol size.

**Table 3.** Matrix correlation (Pearson,  $p < 0.05$  significance level, labeled by asterisk) of element concentrations in aqueous solutions during freezing (left) and thawing (right) of peat leachates. Experiments, with and without insulant, are combined together.

Freezing WSL + F WSL + BZT					Thawing WSL + F WSL + BZT				
	DOC	Na	Al	Fe		DOC	Na	Al	Fe
DOC	1	−0.0584	0.9752 *	0.9537 *	DOC	1	0.1815	0.9320 *	0.9695 *
Li	0.2841	0.6957	0.4028	0.4249	Li	0.9149 *	0.3597	0.9141 *	0.9396 *
B	0.0137	0.9399 *	0.0984	0.1099	B	0.2050	0.9889 *	0.1702	0.2581
Na	−0.0584	1	0.0585	0.0556	Na	−0.4262	1	0.1483	0.2255
Mg	0.2708	0.7249 *	0.3661	0.3465	Mg	0.6507	0.5771	0.6468	0.6935
Al	0.9752 *	0.0585	1	0.9714 *	Al	0.9320 *	0.1483	1	0.9684 *
Si	0.9433 *	0.0777	0.9784 *	0.9533 *	Si	0.9302 *	0.2209	0.9686 *	0.9516 *
P	0.8843 *	0.2769	0.9342 *	0.9110 *	P	0.9797 *	0.1920	0.9584 *	0.9802 *
K	0.8286 *	0.0625	0.8723 *	0.8240 *	K	0.8810 *	0.1027	0.9076 *	0.8650 *
Ca	0.2949	0.7511 *	0.3536	0.4123	Ca	0.6472	0.7605 *	0.6221	0.6901
Ti	0.9329 *	0.1386	0.9767 *	0.9448 *	Ti	0.9463 *	0.3545	0.8872 *	0.9503 *
V	−0.0965	−0.0566	−0.1673	0.0424	V	0.2062	−0.0739	0.2954	0.3317
Cr	0.7382 *	−0.0688	0.7430 *	0.6332	Cr	0.8028 *	0.5378	0.7283 *	0.7761 *
Mn	−0.3950	−0.2971	−0.4310	−0.3443	Mn	−0.4973	−0.2645	−0.3969	−0.4086
Fe	0.9537 *	0.0556	0.9714 *	1	Fe	0.9695 *	0.2254	0.9684 *	1
Co	0.5802	0.2920	0.6675	0.6908	Co	0.8884 *	0.1750	0.9240 *	0.9248 *
Ni	0.7402 *	−0.1376	0.7681 *	0.7031 *	Ni	0.9220 *	0.2549	0.9012 *	0.9375 *
Cu	0.9422 *	0.0668	0.9787 *	0.9200 *	Cu	0.9824 *	0.2509	0.9490 *	0.9864 *
Zn	0.3588	0.3950	0.3647	0.3455	Zn	0.2217	0.8124 *	0.1310	0.2148
Ga	0.9447 *	−0.0082	0.9617 *	0.8982 *	Ga	0.8970 *	0.1903	0.9884 *	0.9363 *
As	0.7844 *	−0.0093	0.7550 *	0.8698 *	As	0.9210 *	0.2233	0.9128 *	0.9598 *
Rb	0.7832 *	−0.1507	0.8052 *	0.7907 *	Rb	0.7769 *	−0.1060	0.9331 *	0.8367 *
Sr	−0.1877	0.5511	−0.1361	−0.0676	Sr	−0.0097	−0.1975	−0.0006	−0.0246
Y	0.8549 *	0.0521	0.8609 *	0.8934 *	Y	0.9522 *	0.3111	0.9301 *	0.9605 *
Zr	0.8053 *	0.0260	0.8602 *	0.7922 *	Zr	0.9661 *	0.2834	0.9565 *	0.9804 *
Nb	0.9546 *	0.1243	0.9925 *	0.9635 *	Nb	0.9577 *	0.3725	0.8911 *	0.9628 *
Mo	−0.5612	0.2892	−0.4798	−0.5046	Mo	−0.4110	−0.2568	−0.3710	−0.4251
Cd	−0.3985	−0.1202	−0.3732	−0.3835	Cd	−0.5188	−0.3213	−0.4304	−0.4827
Sb	−0.5286	0.1542	−0.4595	−0.4747	Sb	−0.3971	−0.2852	−0.3401	−0.3979
Cs	0.6519	−0.1790	0.6329	0.6351	Cs	0.6829	−0.0942	0.8846 *	0.7569 *
Ba	0.4225	−0.1811	0.4279	0.4552	Ba	0.7095 *	−0.0895	0.7918 *	0.7180 *
La	0.6586	−0.0468	0.6731	0.6531	La	0.9526 *	0.1168	0.9755 *	0.9722 *
Ce	0.6706	−0.0138	0.6699	0.6963	Ce	0.9631 *	0.1622	0.9812 *	0.9906 *
Nd	0.9474 *	0.0619	0.9602 *	0.9655 *	Nd	0.9643 *	0.2661	0.9659 *	0.9818 *
Hf	0.7619 *	0.0501	0.8238 *	0.7434 *	Hf	0.9608 *	0.3444	0.9306 *	0.9613 *
Pb	0.9462 *	0.0543	0.9799 *	0.9318 *	Pb	0.9271 *	0.1359	0.9964 *	0.9687 *
Th	0.9580 *	0.0672	0.9842 *	0.9479 *	Th	0.9781 *	0.1818	0.9742 *	0.9873 *
U	0.3306	0.4467	0.3885	0.3045	U	0.6095	0.5018	0.4967	0.5296

Further insights regarding the group of elemental patterns during freezing and thawing were obtained via consideration of correlations between element distribution factors ( $K_d$  solution/ice), as listed in Table 4. These correlations generally confirmed the group of elements described above; i.e., non-conservative, such as DOC, Fe, Al, trace metals, and notably trivalent and tetravalent hydrolysates; and conservative major cations (Na, Ca, Mg) and some anions (B). Overall, the number of significant correlations for  $K_d$  values was lower than that for concentration values, and the maximal number of inter-correlated elements was observed in the thawing experiments.

**Table 4.** Matrix correlation (Pearson,  $p < 0.05$  significance level, labeled by asterisk) of element distribution coefficient ( $K_d$ ) between the aqueous solution and ice during the freezing (left) and thawing (right) of peat leachates. Experiments, with and without insulant, are combined together.

Freezing WSL + F WSL + BZT (Insulant + No Insulant)						Thawing WSL + F WSL + BZT					
	DOC	Na	Al	Ca	Fe		DOC	Na	Al	Ca	Fe
DOC	1	−0.4156	0.5072	0.0843	0.5100	DOC	1	−0.3016	0.5712	0.1688	0.6304
Li	−0.1530	0.7967 *	0.4767	0.7761 *	0.4696	Li	0.2761	−0.0676	0.4645	0.3155	0.3766
B	−0.0739	0.6382	0.0415	0.6214	0.1158	B	−0.0679	0.9436 *	−0.0395	0.7411 *	0.1240
Na	−0.4156	1	0.1041	0.7425 *	0.1953	Na	−0.3016	1	−0.1697	0.5711	−0.0609
Mg	−0.2679	0.8074 *	0.1838	0.7995 *	0.1953	Mg	−0.2314	−0.0126	−0.1526	−0.7061	−0.2045
Al	0.5072	0.1041	1	0.2329	0.7560 *	Al	0.5712	−0.1697	1	0.2742	0.9317 *
Si	0.1082	0.4472	0.5676	0.3854	0.8156 *	Si	0.2021	−0.1342	0.4378	−0.4496	0.3752
P	0.1482	0.4320	0.2525	0.7756 *	0.5143	P	0.7269 *	−0.3039	0.4626	0.2122	0.4140
K	−0.0056	0.3047	0.6187	0.2150	0.4870	K	−0.2479	−0.0247	0.3868	−0.2146	0.2404
Ca	0.0843	0.7425 *	0.2329	1	0.3776	Ca	0.1688	0.5711	0.2742	1	0.4163
Ti	0.5325	0.1927	0.7393 *	0.3701	0.8923 *	Ti	0.4915	−0.0464	0.7842 *	0.4037	0.8648 *
V	0.7352 *	−0.1233	0.4677	0.3208	0.7364 *	V	0.5676	0.0204	0.8124 *	0.6671	0.9248 *
Cr	0.3214	−0.2685	0.3539	−0.1761	−0.1111	Cr	0.1342	0.0799	0.0982	0.2944	0.0721
Mn	−0.0527	−0.1320	0.4663	−0.3944	0.1574	Mn	−0.2300	0.4363	0.4854	0.2417	0.5073
Fe	0.5100	0.1953	0.7560 *	0.3776	1	Fe	0.6304	−0.0609	0.9317 *	0.4163	1
Co	0.0272	0.4662	0.7655 *	0.2426	0.5674	Co	−0.1855	0.0481	0.5476	−0.0876	0.4929
Ni	0.0342	−0.3260	−0.2851	−0.2410	−0.0968	Ni	0.6660	−0.0068	0.6953	0.3143	0.8425 *
Cu	−0.1651	0.3935	0.5024	0.1072	0.6297	Cu	0.2010	−0.1413	0.2787	0.1113	0.1933
Zn	−0.1390	0.0970	0.2811	−0.2016	0.1828	Zn	−0.4330	0.1063	−0.1833	−0.6541	−0.2768
Ga	0.5550	−0.2729	0.4173	0.0082	0.0492	Ga	0.5962	−0.2789	0.5572	−0.0347	0.4060
As	0.7066 *	−0.0685	0.3519	0.3874	0.6971	As	0.5922	−0.0274	0.8507 *	0.5036	0.8904 *
Rb	0.2731	−0.1322	0.6126	−0.0054	0.3259	Rb	0.5634	−0.3121	0.9508 *	0.1782	0.8402 *
Sr	−0.1735	0.7653 *	0.2376	0.8512 *	0.2824	Sr	−0.2950	−0.0756	0.1700	−0.3811	−0.0417
Y	0.1877	0.1517	0.5959	0.1345	0.6976	Y	0.5229	0.0566	0.9368 *	0.3604	0.9358 *
Zr	0.3338	−0.0874	0.4281	0.0913	0.3792	Zr	0.6300	−0.0906	0.9480 *	0.4148	0.9705 *
Nb	0.0318	0.5789	0.7029 *	0.4167	0.7073 *	Nb	0.0933	0.1119	0.6551	0.0888	0.7199 *
Mo	0.5238	0.2488	0.9165 *	0.4235	0.8317 *	Mo	0.0401	0.1440	0.6823	0.0976	0.6416
Cd	−0.0607	−0.1219	0.4597	−0.3656	0.2252	Cd	0.2183	−0.1742	0.8165 *	0.0156	0.8099 *
Sb	0.3598	−0.0489	0.4976	0.1477	0.5904	Sb	0.1665	−0.1549	0.5969	−0.0309	0.4949
Cs	0.5773	−0.2419	0.5398	0.0382	0.3247	Cs	0.5899	−0.2591	0.9123 *	0.2353	0.7915 *
Ba	−0.2300	0.0473	0.1627	−0.2749	0.0073	Ba	−0.3542	−0.0635	0.0718	−0.6617	−0.0606
La	−0.0399	−0.1035	−0.2501	−0.1054	−0.1870	La	0.5587	−0.1475	0.9793 *	0.2546	0.9591 *
Ce	0.1158	−0.0381	0.0226	0.0197	−0.0057	Ce	0.6383	−0.1569	0.9644 *	0.3963	0.9670 *
Pr	0.2602	−0.0751	0.1179	0.0857	0.1968	Pr	0.6663	−0.0715	0.9459 *	0.4638	0.9769 *
Nd	0.3362	0.0534	0.2615	0.2513	0.4887	Nd	0.6476	−0.0423	0.9222 *	0.5276	0.9306 *
Sm	0.4565	−0.1096	0.7472 *	−0.0797	0.6653	Sm	0.5272	0.0892	0.8231 *	0.3027	0.8126 *
Gd	0.2701	−0.0438	0.4191	0.0736	0.4928	Gd	0.5253	−0.2441	0.9277 *	0.2001	0.8383 *
Dy	0.3761	0.0351	0.4851	0.1995	0.7265 *	Dy	0.4651	0.0003	0.8763 *	0.2797	0.9322 *
Yb	0.2059	0.1526	0.5809	0.1827	0.5640	Yb	0.2427	0.2509	0.6487	0.2005	0.6722
Hf	0.2560	−0.0663	0.4668	0.0583	0.2919	Hf	0.5711	0.0393	0.8259 *	0.3117	0.8759 *
W	−0.0986	0.4389	−0.0700	0.4516	0.0428	W	−0.3747	0.7092 *	0.1301	0.3248	0.1942
Pb	−0.1740	0.1610	0.4887	−0.1852	0.2997	Pb	0.4775	−0.2282	0.8482 *	0.1417	0.7263 *
Th	0.6065	0.1494	0.5774	0.5807	0.7874 *	Th	0.5951	−0.1594	0.9138 *	0.4679	0.9234 *
U	0.2473	0.2469	0.6766	0.3174	0.5078	U	−0.2065	0.3369	0.1920	−0.0993	0.0739

#### 4. Discussion

During freezing of natural porewaters that present in the permafrost peatlands, the solutes are known to be excluded downwards during the autumn freeze-up, when the freezing front propagates from the surface to the bottom of the peat profile [54,55]. During this process, the solutes can be accumulated by a factor of ten to hundreds of times in the remaining unfrozen part of the porewaters in mineral and organic soils [54,56,57]. The basic mechanism of DOC and inorganic solute accumulation in the residual fluid during ice formation in the reactor is simply a physically induced increase in their concentration

at the freezing front propagation [58,59]. Numerous experiments on homogeneous and heterogeneous aqueous–solid systems demonstrated that the impurities (present in the form of soluble salts or suspended materials) are separated from aqueous solution by the so-called dynamic freezing front [60,61]. Other experiments on the freezing of natural surface waters of Arctic peatlands, similar to the peat porewater of the current study, demonstrated a progressive freezing of water from the reactor edges to the center, accompanied by the relative accumulation of DOM in the remaining liquid [46,53].

The temporal concentration patterns and elemental correlations demonstrated two contrasting group of solutes—labile elements and insoluble elements. The labile elements were present in essentially ionic forms (alkalis, alkaline–earth metals, oxyanions, and neutral molecules) which did not correlate with DOC, Fe, and Al, and exhibited rather similar concentrations in the fluid prior to freezing and after the entire freeze–thaw sequence. Contrasting to these soluble and labile solutes were divalent metals and insoluble  $TE^{3+}$  and  $TE^{4+}$  trace elements, which are known to be carried in the form of organic and organo-mineral (Fe, Al) colloids in the peat porewater (i.e., [15]) and dispersed ice of the peat cores [10]. Therefore, in agreement with previous studies of experimental bi-directional freezing of the entire peat cores (i.e., [44,45]), we hypothesize that, during freezing front propagation, large size organic-Fe-Al colloids are subjected to preferential exclusion relative to truly dissolved (inorganic) solutes from the ice. As a result, they could form precipitates either in the bulk of the remaining fluid or at the actual interface between the forming ice and the remaining aqueous solution.

It is known that high DOM concentrations diminish the proportion of DOC incorporated into the ice phase [20,62,63]. In the present study, we observed a positive correlation ( $R = 0.94$ ,  $p < 0.01$ ) between the initial DOC concentration in the leachates and the  $K_d$  value of DOC. Note however, that a rather high concentration of initial DOM and a fast freezing rate (at  $-20\text{ }^{\circ}\text{C}$ ) could drive some parts of ionic solutes and even organic colloids to be occluded in the bulk of developing ice in the form of liquid pockets, as is known for sea ice formation [64], and has been recently demonstrated for mineral soils [65,66].

Some decrease in DOM between the initial leachate and final fluid, after full freezing and thawing, is most likely linked to coagulation, precipitation, and removal (on filters) in the form of amorphous organic-rich solid phases. The detailed molecular mechanisms of this freeze-induced coagulation of ionic solutes and colloids are not known [35,45,46]. The chemical nature of coagulated material has not been investigated in the present study, but most likely includes, in addition to organic humic particles (e.g., [67]), organo-mineral composites of Fe and Al (hydr)oxides tightly linked to organic matter (OM). Such complex compounds are primary carriers of trace metal in soils and groundwater [68–70], as also evidenced by studies of colloidal matter in the surface waters of permafrost peatlands [10,14,15,71].

Despite these measurable, but rather minor, decreases in some component concentrations between the initial leachate and the final fluid obtained after the full freezing and thawing of the reactors, the present study generally evidenced a good recovery of DOC and most solutes over reversible freezing and thawing cycles. The results of the present study thus corroborate those reported earlier regarding the rather minor (i.e., <10–30%) effects of freeze–thaw cycles on DOC quantity and quality in acidic peat leachates [46]. Overall, this demonstrates the high stability of dissolved (<0.45  $\mu\text{m}$ ) OC, Fe, Al, and some trace metals to the repetitive freezing and thawing of surface waters in permafrost peatlands.

## 5. Conclusions

Experimental modeling of the reversible freezing and thawing of the aqueous leachates of peat originating from permafrost peatlands demonstrated a systematic evolution of the solute concentration of remaining/forming fluids in the course of progressive freezing/thawing, respectively. Element partitioning between the initial filtrate and the one formed after complete freezing and thawing varied, depending on the nature of the element and its relative affinity to organic matter, Fe/Al hydroxide colloids, or simple ionic

complexes. In accord with the first hypothesis of this study, we revealed two groups of solutes: (1) those incorporating into forming ice; and (2) those remaining in the fluid phase via concentration due to freezing front migration, but not subjected to coagulation. In contrast, we did not note the existence of insoluble organo-mineral amorphous compounds or minerals subjected to irreversible coagulation. A likely reason for the latter observation is the rather acidic pH of peat leachates and high DOC concentrations, leading to the stabilization of typically insoluble solid phases known to be subjected to cryo-induced precipitation, such as Fe, Al hydroxide, or Ca carbonate minerals.

The leachates of frozen peat behaved drastically differently from the leachates of peat from the active layer, as the concentration of DOC, Fe and other solutes in the remaining fluid did not increase upon progressive freezing. We thus demonstrate the efficient incorporation of solutes from frozen peat leachates into the forming ice, as reflected by quite low partitioning coefficients of elements between forming ice and the remaining fluid for this type of substrate. It is thus possible that some volumes of the fluid, formed from frozen leachate, partially preserved the peat-dispersed ice structure and chemical composition and could be directly incorporated into forming ice, with a partitioning coefficient close to 1.

We also conclude that one can use a laboratory leachate of natural substrates, such as peat, as a surrogate for the direct experimental modeling of chemical and physical processes occurring in permafrost peatlands during the autumn—spring period. Overall, the present study provides a solid experimental basis for constructing a uniform approach for the laboratory modeling of soil fluid behavior in permafrost peatlands.

**Author Contributions:** Conceptualization, I.S.I. and O.S.P.; field sampling, I.S.I. and L.S.S.; analysis of collected samples, J.-L.R., I.S.I. and L.S.S.; experiments, I.S.I. and O.S.P.; visualization, I.S.I.; writing and editing O.S.P., I.S.I., L.S.S. and J.-L.R. All authors have read and agreed to the published version of the manuscript.

**Funding:** The study was funded by the Ministry of Education and Science of the Russian Federation (Agreement No. 075-15-2022-241).

**Institutional Review Board Statement:** Not applicable.

**Informed Consent Statement:** Not applicable.

**Data Availability Statement:** Not applicable.

**Conflicts of Interest:** The authors declare no conflict of interest.

## References

1. Henry, H.A.L. Climate change and soil freezing dynamics: Historical trends and projected changes. *Clim. Change* **2008**, *87*, 421–434. [\[CrossRef\]](#)
2. Hayashi, M. The cold vadose zone: Hydrological and ecological significance of frozen-soil processes. *Vadose Zone J.* **2013**, *12*, 1–8. [\[CrossRef\]](#)
3. Shogren, A.J.; Zarnetske, J.P.; Abbott, B.W.; Iannucci, F.; Bowden, W.B. We cannot shrug off the shoulder seasons: Addressing knowledge and data gaps in an Arctic headwater. *Environ. Res. Lett.* **2020**, *15*, 104027. [\[CrossRef\]](#)
4. Manasypov, R.M.; Vorobyev, S.N.; Loiko, S.V.; Kritzkov, I.V.; Shirokova, L.S.; Shevchenko, V.P.; Kirpotin, S.N.; Kulizhsky, S.P.; Kolesnichenko, L.G.; Zemtsov, V.A.; et al. Seasonal dynamics of organic carbon and metals in thermokarst lakes from the discontinuous permafrost zone of western Siberia. *Biogeosciences* **2015**, *12*, 3009–3028. [\[CrossRef\]](#)
5. Pokrovsky, O.S.; Manasypov, R.M.; Kopysov, S.G.; Krickov, I.V.; Shirokova, L.S.; Loiko, S.V.; Lim, A.G.; Kolesnichenko, L.G.; Vorobyev, S.N.; Kirpotin, S.N. Impact of permafrost thaw and climate warming on riverine export fluxes of carbon, nutrients and metals in Western Siberia. *Water* **2020**, *12*, 1817. [\[CrossRef\]](#)
6. Krickov, I.V.; Lim, A.G.; Shevchenko, V.P.; Starodymova, D.P.; Dara, O.M.; Kolesnichenko, Y.; Zinchenko, D.O.; Vorobyev, S.N.; Pokrovsky, O.S. Seasonal Variations of Mineralogical and Chemical Composition of Particulate Matter in a Large Boreal River and Its Tributaries. *Water* **2023**, *15*, 633. [\[CrossRef\]](#)
7. Ma, Q.; Jin, H.; Yu, C.; Bense, V.F. Dissolved organic carbon in permafrost regions: A review. *Sci. China Earth Sci.* **2019**, *62*, 349–364. [\[CrossRef\]](#)
8. Vonk, J.E.; Tank, S.E.; Bowden, W.B.; Laurion, I.; Vincent, W.F.; Alekseychik, P.; Amyot, M.; Billet, M.F.; Canario, J.; Cory, R.M.; et al. Reviews and syntheses: Effects of permafrost thaw on Arctic aquatic ecosystems. *Biogeosciences* **2015**, *12*, 7129–7167. [\[CrossRef\]](#)

9. Lim, A.G.; Loiko, S.V.; Kuzmina, D.M.; Krickov, I.V.; Shirokova, L.S.; Kulizhsky, S.P.; Vorobyev, S.N.; Pokrovsky, O.S. Dispersed ground ice of permafrost peatlands: A non-accounted for source of C, nutrients and metals. *Chemosphere* **2021**, *226*, 128953. [[CrossRef](#)]
10. Lim, A.G.; Loiko, S.V.; Kuzmina, D.M.; Shirokova, L.S.; Pokrovsky, O.S. Organic carbon, and major and trace elements reside in labile low-molecular form in the ground ice of permafrost peatlands: A case study of colloids in peat ice of Western Siberia. *Environ. Sci. Process. Impacts* **2022**, *24*, 1443–1459. [[CrossRef](#)]
11. Fu, Z.; Wu, Q.; Zhang, W.; He, H.; Wang, L. Water migration and segregated ice formation in frozen ground: Current advances and future perspectives. *Front. Earth Sci.* **2022**, *10*, 826961. [[CrossRef](#)]
12. Reeve, A.S.; Siegel, D.I.; Glaser, P.H. Geochemical controls on peatland pore water from the Hudson Bay Lowland: A multivariate statistical approach. *J. Hydrol.* **1996**, *181*, 285–304. [[CrossRef](#)]
13. Raudina, T.V.; Loiko, S.V.; Lim, A.G.; Krickov, I.V.; Shirokova, L.S.; Istigechev, G.I.; Kuzmina, D.M.; Kulizhsky, S.P.; Vorobyev, S.N.; Pokrovsky, O.S. Dissolved organic carbon and major and trace elements in peat porewater of sporadic, discontinuous, and continuous permafrost zones of western Siberia. *Biogeosciences* **2017**, *14*, 3561–3584. [[CrossRef](#)]
14. Pokrovsky, O.S.; Manasypov, R.M.; Loiko, S.V.; Shirokova, L.S. Organic and organo-mineral colloids in discontinuous permafrost zone. *Geochim. Cosmochim. Acta* **2016**, *188*, 1–20. [[CrossRef](#)]
15. Raudina, T.V.; Loiko, S.V.; Kuzmina, D.M.; Shirokova, L.S.; Kulizhsky, S.P.; Golovatskaya, E.A.; Pokrovsky, O.S. Colloidal organic carbon and trace elements in peat porewaters across a permafrost gradient in Western Siberia. *Geoderma* **2021**, *390*, 114971. [[CrossRef](#)]
16. DeLuca, T.H.; Keeney, D.R.; McCarty, G.W. Effect of freeze-thaw events on mineralization of soil nitrogen. *Biol. Fertil. Soils* **1992**, *14*, 116–120. [[CrossRef](#)]
17. Dietzel, M. Impact of cycling freezing on precipitation of silica in Me-SiO<sub>2</sub>-H<sub>2</sub>O systems and geochemical implications for cryosols and sediments. *Chem. Geol.* **2005**, *216*, 79–88. [[CrossRef](#)]
18. Du, L.; Dyck, M.; Shoty, W.; He, H.; Lv, J.; Cuss, C.; Bie, J. Lead immobilization processes in soils subjected to freeze-thaw cycles. *Ecotoxicol. Environ. Saf.* **2020**, *192*, 110288. [[CrossRef](#)]
19. Fitzhugh, R.D.; Driscoll, C.T.; Groffman, P.M.; Tierney, G.L.; Fahey, T.J.; Hardy, J.P. Soil freezing and the acid-base chemistry of soil solutions in a northern hardwood forest. *Soil Sci. Soc. Am. J.* **2003**, *67*, 1897–1908. [[CrossRef](#)]
20. Hentschel, K.; Borcken, W.; Matzner, E. Repeated freeze–thaw events affect leaching losses of nitrogen and dissolved organic matter in a forest soil. *J. Plant. Nutr. Soil Sci.* **2008**, *171*, 699–706. [[CrossRef](#)]
21. Kim, E.-A.; Lee, H.K.; Choi, J.H. Effects of a controlled freeze-thaw event on dissolved and colloidal soil organic matter. *Environ. Sci. Pollut. Res.* **2017**, *24*, 1338–1346. [[CrossRef](#)] [[PubMed](#)]
22. Larsen, K.S.; Jonasson, S.; Michelsen, A. Repeated freeze–thaw cycles and their effects on biological processes in two arctic ecosystem types. *Appl. Soil Ecol.* **2002**, *21*, 187–195. [[CrossRef](#)]
23. Leuther, F.; Schlüter, S. Impact of freeze-thaw cycles on soil structure and soil hydraulic properties. *Soil* **2021**, *7*, 179–191. [[CrossRef](#)]
24. Mohanty, S.K.; Saiers, J.E.; Ryan, J.N. Colloid-facilitated mobilization of metals by freeze-thaw cycles. *Environ. Sci. Technol.* **2014**, *48*, 977–984. [[CrossRef](#)]
25. Mohanty, S.K.; Saiers, J.E.; Ryan, J.N. Colloid mobilization in a fractured soil during dry-wet cycles: Role of drying duration and flow path permeability. *Environ. Sci. Technol.* **2015**, *49*, 9100–9106. [[CrossRef](#)]
26. Ren, J.; Vanapalli, S.K. Effect of freeze–thaw cycling on the soil-freezing characteristic curve of five Canadian soils. *Vadose Zone J.* **2020**, *19*, e20039. [[CrossRef](#)]
27. Semenov, V.M.; Kogut, B.M.; Lukin, S.M. Effect of repeated drying-wetting-freezing-thawing cycles on the active soil organic carbon pool. *Eurasian Soil Sci.* **2014**, *47*, 276–286. [[CrossRef](#)]
28. Schimel, J.P.; Clein, J.S. Microbial response to freeze-thaw cycles in tundra and taiga soils. *Soil Biol. Biochem.* **1996**, *28*, 1061–1066. [[CrossRef](#)]
29. Vestgarden, L.S.; Austnes, K. Effects of freeze–thaw on C and N release from soils below different vegetation in a montane system: A laboratory experiment. *Glob. Change Biol.* **2009**, *15*, 876–887. [[CrossRef](#)]
30. Xiao, L.; Zhang, Y.; Li, P.; Xu, G.; Shi, P.; Zhang, Y. Effects of freeze-thaw cycles on aggregate-associated organic carbon and glomalin-related soil protein in natural-succession grassland and Chinese pine forest on the Loess Plateau. *Geoderma* **2019**, *334*, 1–8. [[CrossRef](#)]
31. Zhang, Z.; Ma, W.; Feng, W.; Xiao, D.; Hou, X. Reconstruction of soil particle composition during freeze-thaw cycling: A review. *Pedosphere* **2016**, *26*, 167–179. [[CrossRef](#)]
32. Nagare, R.M.; Schincariol, R.A.; Quinton, W.L.; Hayashi, M. Effects of freezing on soil temperature, freezing front propagation and moisture redistribution in peat: Laboratory investigations. *Hydrol. Earth Syst. Sci.* **2012**, *16*, 501–515. [[CrossRef](#)]
33. Nagare, R.M.; Schincariol, R.A.; Quinton, W.L.; Hayashi, M. Moving the field into the lab: Simulation of water and heat transport in Subarctic Peat. *Permafrost Periglacial Proc.* **2012**, *23*, 237–243. [[CrossRef](#)]
34. Smerdon, B.D.; Mendoza, C.A. Hysteretic freezing characteristics of riparian peatlands in the Western Boreal Forest of Canada. *Hydrol. Process.* **2010**, *24*, 1027–1038. [[CrossRef](#)]

35. McCarter, C.P.R.; Rezanezhad, F.; Quinton, W.L.; Gharedaghloo, B.; Lennartz, B.; Price, J.; Connon, R.; Van Cappellen, P. Pore-scale controls on hydrological and geochemical processes in peat: Implications on interacting processes. *Earth-Sci. Rev.* **2020**, *207*, 103227. [[CrossRef](#)]
36. Schwamborn, G.; Schirrmeister, L.; Frütsch, F.; Diekmann, B. Quartz weathering in freeze–thaw cycles: Experiment and application to the El’gygytgyn Crater Lake record for tracing Siberian permafrost history. *Geogr. Ann. Ser. A Phys. Geogr.* **2012**, *94*, 481–499. [[CrossRef](#)]
37. Wang, J.Y.; Song, C.C.; Hou, A.X.; Miao, Y.Q.; Yang, G.S.; Zhang, J. Effects of freezing thawing cycle on peatland active organic carbon fractions and enzyme activities in the Da Xing’anling Mountains, Northeast China. *Environ. Earth Sci.* **2014**, *72*, 1853–1860. [[CrossRef](#)]
38. Chen, J.; Xue, S.; Lin, Y.; Wang, C.; Wang, Q.; Han, Q. Effect of freezing–thawing on dissolved organic matter in water. *Desalination Water Treat.* **2016**, *57*, 17230–17240. [[CrossRef](#)]
39. Fellman, J.B.; D’Amore, D.V.; Hood, E. An evaluation of freezing as a preservation technique for analyzing dissolved organic C, N and P in surface water samples. *Sci. Total Environ.* **2008**, *392*, 305–312. [[CrossRef](#)]
40. Jiang, N.; Juan, Y.; Tian, L.; Chen, X.; Sun, W.; Chen, L. Modification of the composition of dissolved nitrogen forms, nitrogen transformation processes, and diversity of bacterial communities by freeze–thaw events in temperate soils. *Pedobiologia* **2018**, *71*, 41–49. [[CrossRef](#)]
41. Kim, E.-A.; Choi, J.H. Changes in the mineral element compositions of soil colloidal matter caused by a controlled freeze-thaw event. *Geoderma* **2018**, *318*, 160–166. [[CrossRef](#)]
42. Chung, H.Y.; Jung, J.; Lee, D.H.; Kim, S.; Lee, M.K.; Lee, J.I.; Yoo, K.-C.; Lee, Y.I.; Kim, K. Chemical weathering of granite in ice and its implication for weathering in polar regions. *Minerals* **2020**, *10*, 185. [[CrossRef](#)]
43. Savenko, A.V.; Savenko, V.S.; Pokrovsky, O.S. Phase fractionation of chemical elements during the formation of ice in fresh surface waters. *Doklady Acad. Sci. Ser. Earth Sci. Geogr.* **2020**, *492*, 48–54. [[CrossRef](#)]
44. Morgalev, S.Y.; Morgaleva, T.G.; Morgalev, Y.N.; Loiko, S.V.; Manasypov, R.M.; Lim, A.G.; Pokrovsky, O.S. Experimental modeling of the bacterial community translocation during freezing and thawing of peat permafrost soils of Western Siberia. *IOP Conf. Ser. Earth Environ. Sci.* **2019**, *400*, 012017. [[CrossRef](#)]
45. Morgalev, S.Y.; Lim, A.G.; Morgaleva, T.G.; Morgalev, Y.N.; Manasypov, R.M.; Kuzmina, D.M.; Shirokova, L.S.; Orgogozo, L.; Loiko, S.V.; Pokrovsky, O.S. Fractionation of organic C, nutrients, metals and bacteria in peat porewater and ice after freezing and thawing. *Environ. Sci. Pollut. Res.* **2023**, *30*, 823–836. [[CrossRef](#)]
46. Payandi-Rolland, D.; Shirokova, L.S.; Labonne, F.; Bénézeth, P.; Pokrovsky, O.S. Low impact of freeze-thaw cycles on organic carbon and metals in waters of permafrost peatlands. *Chemosphere* **2021**, *279*, 130510. [[CrossRef](#)]
47. Shirokova, L.S.; Chupakov, A.V.; Zabelina, S.A.; Neverova, N.V.; Payandi-Rolland, D.; Causseraund, C.; Karlsson, J.; Pokrovsky, O.S. Humic surface waters of frozen peat bogs (permafrost zone) are highly resistant to bio- and photodegradation. *Biogeosciences* **2019**, *16*, 2511–2526. [[CrossRef](#)]
48. Shirokova, L.S.; Chupakov, A.V.; Ivanova, I.S.; Moreva, O.Y.; Zabelina, S.A.; Shutskiy, N.A.; Loiko, S.V.; Pokrovsky, O.S. Lichen, moss and peat control of C, nutrient and trace metal regime in lakes of permafrost peatlands. *Sci. Total Environ.* **2021**, *782*, 146737. [[CrossRef](#)]
49. Morgalev, Y.N.; Lushchaeva, I.V.; Morgaleva, T.G.; Kolesnichenko, L.G.; Loiko, S.V.; Krickov, I.V.; Lim, A.G.; Raudina, T.V.; Volkova, I.I.; Shirokova, L.S.; et al. Bacteria primarily metabolize at the active layer/permafrost border in the peat core from a permafrost region in western Siberia. *Polar Biol.* **2017**, *40*, 1645–1659. [[CrossRef](#)]
50. Aksenov, A.S.; Shirokova, L.S.; Kisil, O.Y.; Kolesova, S.N.; Lim, A.G.; Kuzmina, D.M.; Pouille, S.; Alexis, M.A.; Castrec-Rouelle, M.; Loiko, S.V.; et al. Bacterial number and genetic diversity in a permafrost peatland (western Siberia): Testing a link with organic matter quality and elementary composition of a peat soil profile. *Diversity* **2021**, *13*, 328. [[CrossRef](#)]
51. Heimbürger, A.; Tharaud, M.; Monna, F.; Losno, R.; Desboeufs, K.; Nguyen, E. SLRS-5 elemental concentrations deduced from SLRS-5/SLRS-4 ratios of thirty-three uncertified elements. *Geostand. Geoanal. Res.* **2013**, *37*, 77–85. [[CrossRef](#)]
52. Yeghicheyan, D.; Bossy, C.; Bouhnik Le Coz, M.; Douchet, C.; Granier, G.; Heimbürger, A.; Lacan, F.; Lanzanova, A.; Rousseau, T.C.C.; Seidel, J.-L.; et al. A compilation of silicon, rare earth element and twenty-one other trace element concentrations in the natural river water Reference Material SLRS-5 (NRC-CNRC). *Geostand. Geoanal. Res.* **2013**, *37*, 449–467. [[CrossRef](#)]
53. Pokrovsky, O.S.; Karlsson, J.; Giesler, R. Freeze-thaw cycles of Arctic thaw ponds remove colloidal metals and generate low-molecular-weight organic matter. *Biogeochemistry* **2018**, *137*, 321–336. [[CrossRef](#)]
54. Kokelj, S.V.; Burn, C.R. Geochemistry of the active layer and near-surface permafrost, Mackenzie delta region, Northwest Territories, Canada. *Can. J. Earth Sci.* **2005**, *42*, 37–48. [[CrossRef](#)]
55. French, H.; Shur, Y. The principles of cryostratigraphy. *Earth-Sci. Rev.* **2010**, *101*, 190–206. [[CrossRef](#)]
56. Lamhonwah, D.; Lafrenière, M.J.; Lamoureux, S.F.; Wolfe, B.B. Multi-year impacts of permafrost disturbance and thermal perturbation on High Arctic stream chemistry. *Arct. Sci.* **2016**, *3*, 254–276. [[CrossRef](#)]
57. Lamhonwah, D.; Lafrenière, M.J.; Lamoureux, S.F.; Wolfe, B.B. Evaluating the hydrological and hydrochemical responses of a High Arctic catchment during an exceptionally warm summer. *Hydrol. Process.* **2017**, *31*, 2296–2313. [[CrossRef](#)]
58. Ewing, S.A.; O’Donnell, J.A.; Aiken, G.R.; Butler, K.; Butman, D.; Windham-Myers, L.; Kanevskiy, M.Z. Long-term anoxia and release of ancient, labile carbon upon thaw of Pleistocene permafrost. *Geophys. Res. Lett.* **2015**, *42*, 10730–10738. [[CrossRef](#)]



59. Ostroumov, V.; Hoover, R.; Ostroumova, N.; Van Vliet-Lanoë, B.; Siegert, C.; Sorokovikov, V. Redistribution of soluble components during ice segregation in freezing ground. *Cold Reg. Sci. Technol.* **2001**, *32*, 175–182. [[CrossRef](#)]
60. Shafique, U.; Anwar, J.; uz-Zaman, W.; Rehman, R.; Salman, M.; Dar, A.; Jamil, N. Forced migration of soluble and suspended materials by freezing front in aqueous systems. *J. Hydro-Environ. Res.* **2012**, *6*, 221–226. [[CrossRef](#)]
61. Takenaka, N.; Bandow, H. Chemical kinetics of reactions in the unfrozen solution of ice. *J. Phys. Chem. A* **2007**, *111*, 8780–8786. [[CrossRef](#)] [[PubMed](#)]
62. Elliott, A.C.; Henry, H.A.L. Freeze–thaw cycle amplitude and freezing rate effects on extractable nitrogen in a temperate old field soil. *Biol. Fertil. Soils.* **2009**, *45*, 469–476. [[CrossRef](#)]
63. Xue, S.; Wen, Y.; Hui, X.; Zhang, L.; Zhang, Z.; Wang, J.; Zhang, Y. The migration and transformation of dissolved organic matter during the freezing processes of water. *J. Environ. Sci.* **2015**, *27*, 168–178. [[CrossRef](#)] [[PubMed](#)]
64. Petrich, C.; Eicken, H. Growth, Structure and Properties of Sea Ice. In *Sea Ice*, 2nd ed.; Thomas, D.N., Dieckmann, G.S., Eds.; Wiley Blackwell: Oxford, UK, 2010; Volume 2, pp. 425–467. [[CrossRef](#)]
65. Chen, C.; Huang, H.; Mo, X.; Xue, H.; Liu, M.; Chen, H. Insights into the kinetic processes of solute migration by unidirectional freezing in porous media with micromodel visualization at the pore-scale. *Sci. Total Environ.* **2021**, *784*, 147178. [[CrossRef](#)]
66. Ju, Z.; Du, Z.; Guo, K.; Liu, X. Irrigation with freezing saline water for 6 years alters salt ion distribution within soil aggregates. *J. Soil Sediments* **2019**, *19*, 97–105. [[CrossRef](#)]
67. Giesy, J.P.; Briese, L.A. Particulate formation due to freezing humic waters. *Water Resour. Res.* **1978**, *14*, 542–544. [[CrossRef](#)]
68. McCarthy, J.F.; Zachara, J.M. Subsurface transport of contaminants. *Environ. Sci. Technol.* **1989**, *23*, 496–502. [[CrossRef](#)]
69. Murphy, E.M.; Zachara, J.M. The role of sorbed humic substances on the distribution of organic and inorganic contaminants in groundwater. *Geoderma* **1995**, *67*, 103–124. [[CrossRef](#)]
70. Otero Farina, A.; Peacock, C.L.; Fiol, S.; Antelo, J.; Carvin, B. A universal adsorption behaviour for Cu uptake by iron (hydr) oxide organo-mineral composites. *Chem. Geol.* **2018**, *479*, 22–35. [[CrossRef](#)]
71. Krickov, I.V.; Pokrovsky, O.S.; Manasyrov, R.M.; Lim, A.G.; Shirokova, L.S.; Viers, J. Colloidal transport of carbon and metals by western Siberian rivers during different seasons across a permafrost gradient. *Geochim. Cosmochim. Acta* **2019**, *265*, 221–241. [[CrossRef](#)]

**Disclaimer/Publisher’s Note:** The statements, opinions and data contained in all publications are solely those of the individual author(s) and contributor(s) and not of MDPI and/or the editor(s). MDPI and/or the editor(s) disclaim responsibility for any injury to people or property resulting from any ideas, methods, instructions or products referred to in the content.